Indian Journal of Science and Technology, *Vol 9(36), DOI: 10.17485/ijst/2016/v9i36/93659, September 2016*
ISSN (Print) : 0974-6846
ISSN (Online) : 0974-5645

Mechanical Characterization of Additive Manufacturing Processes

Mukund Joshi, Nagaraja Shetty*, S. Divakara Shetty, N. L. S. Bharath and Chanakya Varma Surapaneni

Department of Mechanical and Manufacturing Engineering, Manipal Institute of Technology, Manipal University, Manipal-576104, Karnataka, India;
hosadunagaraj@gmail.com, mrj1993@gmail.com, shetty.divakar@manipal.edu, namabharath9900@gmail.com, chanakya261094@gmail.com

Abstract

Objectives: To compare two of the most popular rapid prototyping processes of Stereolithography (SLA) and Selective Laser Sintering (SLS) from a product-based perspective, to help customers analyze them and make a choice between the two. **Methods:** This paper includes the qualitative testing of identical specimens created by SLA and SLS. The specimens are evaluated on the parameters of dimensional accuracy, tensile strength, water absorption, surface roughness, density, Vickers hardness and microscopic defect structure. The outcome of this study aims at helping people to understand SLS and SLA better in terms of the products they create so that it becomes easier for users to make a choice between the two. It also aims at highlighting the above mentioned statistical information about SLA and SLS so that they may be improvised and enhanced in the future. **Findings:** Based on the tests conducted, it was confirmed that the SLA specimens were better than the SLS specimens in the tensile strength, water absorption, surface roughness and density tests. The SLS specimens outperformed the SLA specimens in the dimensional accuracy and Vickers hardness tests. Thus it was concluded that the SLA specimens exhibited better mechanical and physical characteristics than the SLS specimens.

Keywords: Additive Manufacturing, Material Properties, Mechanical Characterization, Rapid Prototyping, SLA, SLS

1. Introduction

Rapid Prototyping (RP) is a term used for a variety of manufacturing processes that fall under the domain of additive manufacturing. RP gains importance in applications where a quick and convenient production is of prime importance[1]. In general, manufacturing can be classified into two categories- subtractive and additive manufacturing. Conventional methods like turning, drilling, shaping, boring, and even advanced processes like water jet cutting, Electrical Discharge Machining (EDM) and Computer Numeric Controlled (CNC) machining fall under the category of 'subtractive manufacturing', in which material is removed from a bigger main workpiece to produce the final finished product. Unlike this methodology, 'additive manufacturing'[2] which includes technologies like rapid prototyping, is a relatively new concept in which material is incrementally added to build the finished product layer by layer.

Since its inception, RP processes have diversified in application[3]. What was initially devised as a method to create quick prototypes of components before investing in a full-scale working model, today finds application in industry, automobiles, aviation, medicine, architecture, cooking and even as an art form[4]. Some examples of the above include the use of RP in wind tunnel modeling[5], in continuous manufacturing[6], tooling[7], medical prosthetics such as wrist implants and prosthetic legs[8], manufacture of photoelastic models[9], architectural prototypes and miniature construction models[10], in aerospace[11] and turbomachinery[12], in dentistry[13], the manufacture of injection molds[14], and the recreation of now obso-

*Author for correspondence

lete technological specimens[15], in reverse engineering[16], Micro Electro Mechanical Systems (MEMS)[17] and nanotechnology[18] among others. Early engineers relied upon handmade drawings and designs to manufacture components, which was replaced by Computer Aided Design (CAD) diagrams and soft-copies of designs and prototype models with the advent of designing and simulation software. While this proved to be a boon as it saved both time and effort, it had its own shortcomings. For example, one cannot perceive a CAD model of a component as clearly as a live 3-dimensional rendition of the same. Also, it would often be difficult for a person not from the designing background to comprehend these CAD designs and models. Rapid prototyping gained importance in manufacturing because it overcame these shortcomings. Prototypes created by RP can be felt with one's hands, and examined in a better manner by the layman. This quality popularized RP as a technology that could be employed to create economic miniature prototypes of otherwise large and complex projects which would be too complicated to be viewed in a software, but too expensive to create in full size.

Over time, various rapid prototyping processes have been developed to satisfy the many needs of customers. These processes are safer and much more time to save than conventional processes[19]. The basic process in any additive manufacturing setup is to add raw material (liquid, powdered or granular) layer by layer and fix it in position by some binding process such as glue, resin, or high temperature[20]. Some of the currently popular RP processes (classified according to the type of Raw Material) are mentioned in Table 1. The various types of RP processes produce products of different qualities and finishes. However, each process can be internally moderated and controlled, to change the output to be given[21]. In any Rapid Prototyping (RP) process, whether taking the material in the form of solid, liquid or powder, the created product quality can be varied by varying its density, its build orientation and a number of slices or layers[22,23]. This can be achieved changing the process parameters of preheating temperature, bed orientation, and laser intensity (if the laser is used)[24–26].

SLA is one of the oldest but most commonly used RP processes. It involves raw material input in the liquid state. The layered manufacturing technology was originally publicized in 1970 and was then patented as Stereolithography[27]. In this method, the given CAD file is segmented into multiple layers before being fed to the SLA machine. An ultraviolet (UV) laser is now focused on a container with photopolymer solution[28]. The laser traces the path of the shape given by the CAD file, thereby hardening that portion of the liquid. After this, the container is lowered and the next layer is printed on top of it. The material buildup is supported by a build platform and/or support structures since it cannot hold itself in position in liquid. One of the advantages of this process is quickness of manufacture. SLA is one of the fastest RP processes, considering the fact that process speed is proportional to the complexity of the part to be manufactured[29]. Its downside is its cost. One gallon of photopolymer resin can cost up to $2500. Also, SLA is highly dependent on supports for manufacturing components.

Table 1. Classification of rapid prototyping processes by raw material used

Raw Material	Process
Liquid Based	Stereolithography (SLA)
	Polyjet
	Liquid Thermal Polymerization (LTP)
	Beam Interference Solidification (BIS)
	Holographic Interference Solidification (HIS)
	Electrosetting (ES)
	3 Dimensional Welding (3DW)
	Shape Deposition Manufacturing (SDM)
	Solid Ground Curing
	Ballistic Particle Manufacturing (BPM)
Solid Based	Laminated Object Manufacturing (LOM)
	Solid Foil Polymerization (SFP)
	Fused Deposition Modeling (FDM)
Powder Based	Selective Laser Sintering (SLS)
	Spatial Forming (SF)
	Gas Phase Deposition (GPS)
	3D Printing (3DP)
	Laser Engineered Net Shaping (LENS)

SLS is one of the most widely used prototyping processes available today[30]. It was developed by the University of Texas at Austin. It involves sintering of raw material along predetermined paths to create the product as per the given CAD file. The difference is that SLS uses powdered raw material instead of liquid. A roller rolls a layer

of powder onto the sintering bed, which is solidified by a laser. The advantage of this process is that the unsintered powder stacks up and suspends the sintered product between itself, this obviating the need for any support structure[31]. It is thus very convenient to manufacture multiple parts in a single run. It is also cheaper than SLA.

This paper aims at comparing two of the most popular rapid prototyping processes. SLA and SLS are widely used for prototyping and limited manufacturing. However, the cost of RP processes is high, which limits its functionality in some ways. To tackle this problem, we need to revolutionize rapid prototyping and make it more accessible, and evaluating the most popular forms of RP greatly benefits the same. This paper aims at comparing identical products created by SLA and SLS on the parameters of dimensional accuracy, tensile strength, water absorption, surface roughness, density, Vickers hardness and microscopic defect structure in order to analyze how the two processes can be improvised[32]. It also gives a first-hand analysis of SLA and SLS helping them to decide the better-suited option for their needs. With the increasing importance of rapid prototyping in today's industrial applications, it has become necessary to quantify all the aspects that govern the quality of solid free formed products[33] The analysis of energy utilization of the laser used in many rapid prototyping applications, which is affected by the parameters of slice thickness and orientation of CAD model[34].

A new approach to the analysis of SLS using Optical Coherence Tomography (OCT) was purely virtual and did not involve actual testing of specimens. All the parameters tested in the above-mentioned works are process specific and not product specific. The researchers elaborate on how to modify the process to get suitable changes in the final product and stated the environmental performance comparison of SLS, SLA and FDM in detail[35–37]. Similarly, compared the processes of SLA, SLS, LOM and FDM-based on the material of use, their advantages and disadvantages, and their price. A genetic algorithm is used to determine optimum part orientation in various rapid prototyping processes. This again can be categorized as a preprocess parameter. Therefore, SLA undergoes lesser shrinkage than SLS during the process, and the shrinkage is easy to predict and correct[38–40]. Finally, Antonio has stressed upon the surface finish, its detection and its effect on parts manufactured by the FDM process[41]. Though this does not pertain to the processes we are concerned with (SLA, SLS), it provides useful insight on one of the most crucial parameters of rapid prototyping.

Rapid prototyping, being a confluence of mechanical, chemical and automation engineering, is influenced by a number of parameters, the common ones including Laser Intensity, Bed pre-heating temperature, laser power, the orientation of the product, slice thickness, the number of slices, the number of parts produced per run, and cycle time[42]. That being said, when a customer has to make a choice between two or more prototyping options to satisfy his needs, his decision would not be based on these parameters. It would rather be based on how strong the components of each process turn out to be, how costly they are, their texture, hardness, and other similar parameters that might be of concern to an end-user.

However, most of the research done in the field of rapid prototyping aim at modifying process variables to produce a more suitable product. The common customer, however, may not relate to this technical nitty-gritty, and will rely on a more direct comparison to evaluate which process yields more favorable results. SLS and SLA are the two most widely used forms of solid free form fabrication. This paper compares the specimens created by SLS and SLA and tested them for parameters of direct importance to the end-user. All our tests are experimental and rely less on virtual hypothesis, thus providing a clear picture of the pros and cons of SLS and SLS. This research will help customers get a clearer picture on which RP process is most suitable to their needs.

2. Methodology

This paper presents comparative testing of identical specimens created by Stereolithography (SLA) and Selective Laser Sintering (SLS) processes, which were manufactured and Imaginarium (India) Pvt. Ltd. Mumbai and tested in the labs at Manipal University, Karnataka, India[41]. The investigations of dimensional accuracy, tensile strength, water absorption, surface roughness and density are presented in this study.

2.1 Experimentation Scheme and Sample Preparation

The manufacture of components was done at Imaginarium (India) Pvt. Ltd. Table 2 shows the specifications of machines used to print the components of SLA and SLS processes. The production was conducted at a temperature of around

32 °C (72 °F) under air conditioning. Laser power for SLA was 500mW and laser intensity for SLS was 42 Watts. The SLA specimens were made from 3D Systems Accura-60 Plastic and the SLS specimens were made from 3D Systems DuraForm PA Plastic[43]. The specimens were manufactured in the horizontal orientation for SLA and SLS processes as shown in Figure 1. The machine used to manufacture the SLA specimens was the 3D Systems Viper Si² machine[44], and the one used to manufacture the SLS specimens was the 3D Systems SinterStation HiQ + HQ machine[45].

Table 2. Details of machines used for SLA and SLS specimen manufacture

Process	Manufacturer	Model	Bed Temperature
SLA	3D Systems	Viper Si²	25 °C
SLS	3D Systems	SinterStation HiQ + HS	172 °C

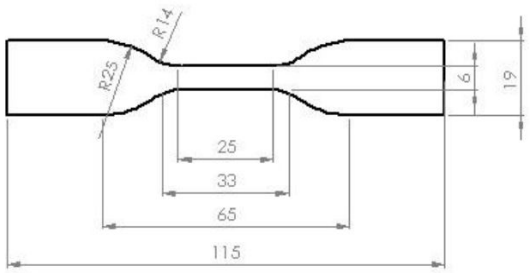

Figure 1. Graphical representation of ASTM D638-10 Type IV specimen with dimensions.

The shape and dimensions of the test specimens were decided according to the ASTM D638-10 standard (Type IV Specimen). The standard recommends at least 5 specimens for testing any particular process parameter. Our tests were conducted at a load rate of 1 mm/min and failure occurred in around 4-5 minutes. The dimensions of the specimen as shown in Table 3.

Table 3. Table of dimensions for ASTM D638-10 Type IV test specimen

ASTM D638-10 Type IV	Dimensions in mm
W (Width of narrow section)	6
L (Length of narrow section)	33
WO (Width overall, min)	19
LO (Length overall, min)	115
G (Gauge length)	25
D (Distance between grips)	65
R (Radius of fillet)	14
RO (Outer radius)	25
T (Thickness)	4

2.2 Dimensional Accuracy Test

Five identical specimens of SLA and SLS each were taken to test their dimensional accuracy as compared to the dimensions of the CAD Model (Modeled after ASTM D638-10 Type IV specifications). The instrument used for measuring dimensions was the Mitutoyo Analog Vernier Caliper with a least count of 0.02 mm. The specimen was cleaned and tested for Overall Length (LO), Overall Width (WO), Width of Narrow Section (W) and Thickness (T) with the caliper (Figure 2). Radii and other dimensions were excluded in the testing for simplicity of operation. The average values of each reading were recorded and the variation of reading was plotted graphically for both SLA and SLS models.

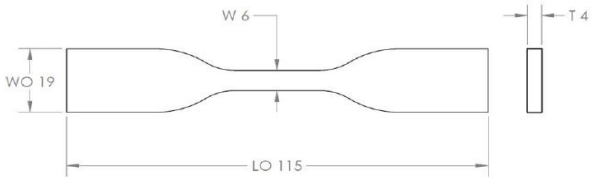

Figure 2. Dimensions considered for the dimensional accuracy test.

2.3 Tensile Strength Test

This test comprised the tensile testing of 5 samples of SLA and SLS each, using the INSTRON 3366 testing machine, which has a 10 kN loading capacity. The gauge length was 25 mm and the specimens were loaded at a rate of 1 mm/min.

The specimen was clamped in the jaws of the machine and it was pulled longitudinally to conduct the tensile test. The tensile stress, tensile strain, and extension were recorded by increasing the load with time. The data obtained was recorded and was also plotted to obtain a stress-strain relationship.

2.4 Water Absorption Test

The water absorption test was conducted to determine the amount of water retained by SLA and SLS specimens when immersed in water. This test was conducted on 5 specimens of SLA and SLS each. To minimize possible error due to environmental and miscellaneous factors, the specimens were wiped clean with a dry cloth and sealed in zip lock air tight bags for one week (168 hours) prior to the testing. The samples were placed in a refrigerator along with silica gel pouches to absorb any residual moisture before conducting the test. When the desired time was reached, the samples were taken out of the zip lock bags and immersed in distilled water in beakers, maintained at approximately 32 °C, for 24 hours. The specimens were weighed before the commencement of the test. After 24 hours, the specimens were wiped with a clean dry cotton cloth and were weighed again. The weighing scale used was the Infra Digital IN 2011 weighing scale. The percentage of water absorbed by the specimens was calculated by the following formula:

$$Percentage\ of\ water\ absorbed = \left\{\frac{Weight\ of\ specimen\ after\ test\ (g) - Initial\ weight(g)}{Initial\ weight(g)}\right\} \times 100 \quad \%$$

2.5 Density Test

The density test was conducted to determine how dense the specimens were, as compared to each other. The knowledge about a specimen's density is useful in analyzing other parameters such as its water absorption, strength, porosity, stiffness and also its ability to withstand warpage due to heat and pressure. The density of specimens was calculated by the Archimedes Principle, which states that a body, when immersed in a liquid, will displace an amount of liquid equal to its own volume. Ten specimens of SLA and SLS each was weighed and the amounts of water they displaced were recorded as well. This was used to calculate their density using the formula:

$$Density = \frac{Mass\ (kg)}{Volume\ (m^3)} \quad kg/m^3$$

2.6 Surface Roughness

Surface Roughness is one of the important tests required for characterizing the quality of a product created by any RP process. Since almost every RP process involves the creation of products by incremental addition of material, the surface of the product is bound to have a stepped/serrated finish. This occurs because every layer of raw material cannot be perfectly aligned with the previously deposited layer of the product. The surface finish of the specimens was calculated using the Mitutoyo Surftest SJ-301 surface roughness testing machine. A diamond-tipped probe was made to travel along the body of the specimen over a range of 4 mm, and the probe recorded variations over the specimen's surface. The machine also provided a graphical response depicting the variation of the surface along the length measured.

2.7 Vickers Hardness Test

The hardness test of composites, plastics and elastomers can be conducted via Vickers hardness test. The knowledge of hardness of rapid prototyping specimens helps us to examine the severity of defection in the specimen's surface on application of force. The test was conducted using 3 specimens of SLA and SLS each. Three readings were taken on each specimen using the Matsuzawa MMT-X7A Vickers hardness testing machine, at locations on the specimen as shown in Figure 3. The readings were calculated and the average hardness of SLA and SLS specimens were calculated and tabulated.

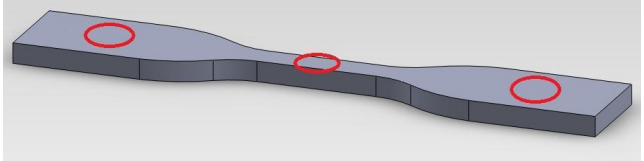

Figure 3. Points for Vickers hardness test on each specimen.

2.8 Microscopy Analysis

Microscopic analysis was conducted on the specimens by observing their structure under a high power microscope. This was done to observe if there were any visible differences in the structure of the SLA and SLS specimens since they were manufactured using different raw materials and processes. The microscope used was the METJI MSHOT M 1004 Trinocular Inverted Metallurgical Microscope. The specimens were cleaned and placed on near the objective lens of the microscope using special fixtures. Images of the specimen's flat surface were recorded at magnifications of 50× and 200×. Also, the specimens that underwent tensile testing were kept under the microscope to observe the nature and type of failure they experienced under tension. In addition to this, the specimens that were subjected to water absorption test were also ana-

lyzed under the microscope to observe the changes in the structure, if any, of the specimens after being immersed in water for 24 hours. Images of the specimens were clicked using the in-built camera and they were used to analyze the properties of the SLA and SLS specimens.

3. Results and Analysis

3.1 Dimensional Accuracy Test

In order to measure tensile properties of the SLA and SLS specimens, the specimens were first subjected to a dimensional accuracy test. The dimensions of the specimens of SLA and SLS each were calculated as shown in Tables 4 and 6, respectively. Their dimensions were used to calculate the dimension change rate and dimensional accuracy using the following formulae:

Table 4. Dimension readings for SLA specimens

SLA	LO	WO	W	T
	L_{SLA}	$B1_{SLA}$	$B2_{SLA}$	H_{SLA}
1	115.2	19	5.96	4.08
2	115	19	5.94	4.02
3	115.3	19	5.96	4.14
4	115	18.96	5.92	4.2
5	115.3	19	5.86	4.14
6	115.1	18.96	5.9	4.08
7	115.1	19	5.92	4.08
8	115	19	5.92	4.1
9	115.18	19.04	5.9	4
10	115.04	18.98	5.96	4.08
11	115	19	5.92	4.04
12	115.02	19	5.72	4.04
13	115.06	18.96	5.82	4.12
14	115.04	18.98	5.92	4.06
15	115.1	19	5.9	4.02

Table 5. Standard deviation, dimensional change rate and dimensional accuracy of SLA

Tests	Std. Deviation (mm)	D. C. R. (%)	D. A. (%)
LO (Overall Length)	0.103978	0.0835	0.0835
WO (Overall Width)	0.021112	-0.042	0.042
W (Width of Narrow Section)	0.062549	-1.644	1.644
T (Thickness)	0.053984	-2.0	2.0

Table 6. Dimension readings for SLS specimens

SLS	LO	WO	W	T
	L_{SLS}	$B1_{SLS}$	$B2_{SLS}$	H_{SLA}
1	115	19	5.98	4.02
2	115	18.9	5.86	3.98
3	115.1	19	5.92	4
4	114.96	19	6	3.98
5	115.18	18.92	5.96	4.12
6	115	19	5.98	4
7	115.8	18.7	6	4.08
8	115.2	19	6	3.96
9	115	18.94	5.98	4.04
10	115	19	5.94	4.08
11	115	18.98	5.98	4.1
12	114.96	19	5.9	4.06
13	114.98	18.94	6	4.04
14	114.76	19	5.98	3.98
15	114.98	18.96	6	4.04

$$Dimensional\ Change\ Rate\,(\%) = \left\{\left[\frac{Measured\ value\ in\ mm}{Desired\ value\ in\ mm}\right] - 1\right\} \times 100$$

$$Dimensional\ Accuracy\,(\%) = \left|\left\{\left[\frac{Measured\ value\ in\ mm}{Desired\ value\ in\ mm}\right] - 1\right\} \times 100\right|$$

The dimensions of Overall Length (LO), Overall Width (WO), Width of Narrow Section (W) and Thickness (T) of the SLA specimens were measured and obtained as shown in Table 5.

The average dimensional accuracy of SLA specimens was found to be 0.94%. The dimensions of Overall Length (LO), Overall Width (WO), Width of Narrow Section (W) and Thickness (T) of the SLS specimens were measured and obtained as shown in Table 6. The average of these readings was determined and used to calculate the standard deviation, Dimensional Change Rate (D. C. R.) and Dimensional Accuracy (D. A.) of each dimension as shown in Table 7. The average dimensional accuracy of SLS specimens was found to be 0.23%.

Figure 4 shows a comprehensive comparison of the 4 dimensions considered in the dimensional accuracy test,

wiz. Overall Length (LO), Overall Width (WO), Width of Narrow Section (W) and Thickness (T), for both, the SLA and SLS Specimens. It can be observed that the dimensional accuracy of SLS specimens is better than that of SLA for all 4 dimensions. Also, a greater error is observed in the smaller dimensions W and T, the error being more in SLA specimens. Figure 5 shows the variation of Overall Length (LO) measurements for the 15 samples of SLA and SLS each. It is observed that the SLA samples have a smaller range of deviation from the expected reading as compared to SLS. SLS shows greater deviation in specimen 8. However, the SLS samples have greater dimensional accuracy. Figure 6 shows the variation of Overall Width (WO) measurements for the 15 samples of SLA and SLS each. A greater consistency in both SLA and SLS readings is observed in this graph with the exception of a few anomalous readings (specimen 10 for SLA and specimens 3, 8 for SLS). Figure 7 shows the variation of Width of Narrow Section (W) measurements for the 15 samples of SLA and SLS each. There is considerable variation in the W measurements of both SLA and SLS specimens, SLA being lesser accurate than SLS in this case.

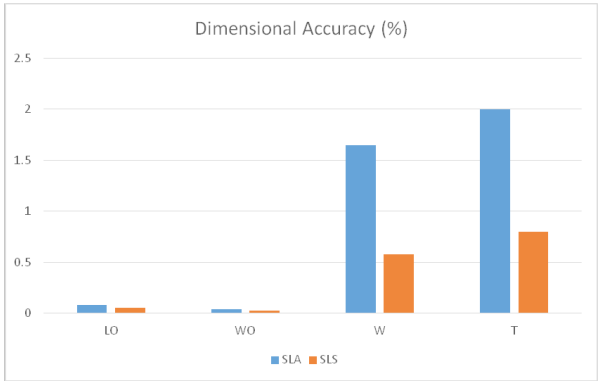

Figure 4. Dimensional accuracy of LO, WO, W, T for SLA and SLS specimens.

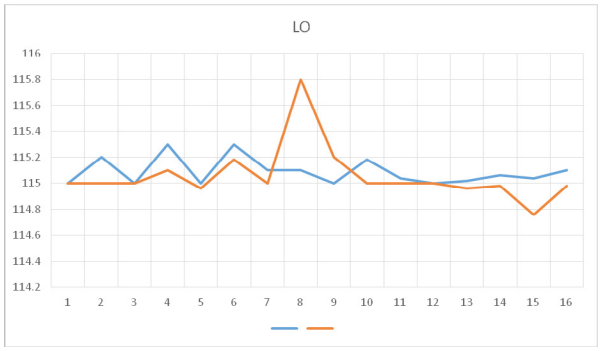

Figure 5. Overall Length of SLA and SLS specimens.

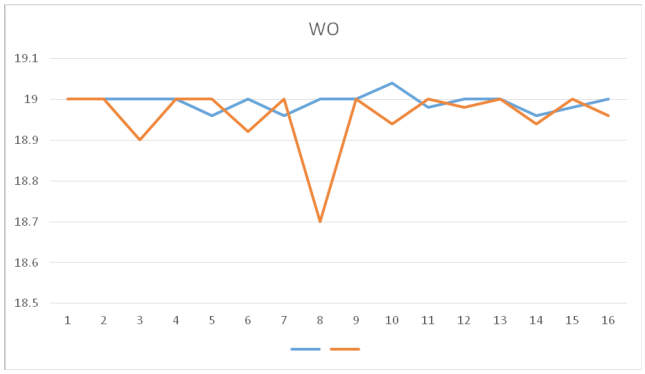

Figure 6. Overall Width of SLA and SLS specimens.

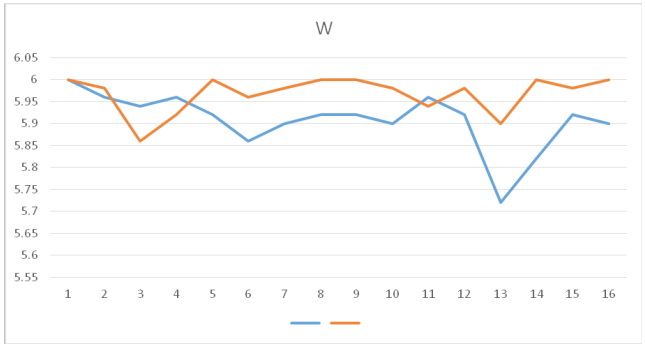

Figure 7. Width of narrow section of SLA and SLS specimens.

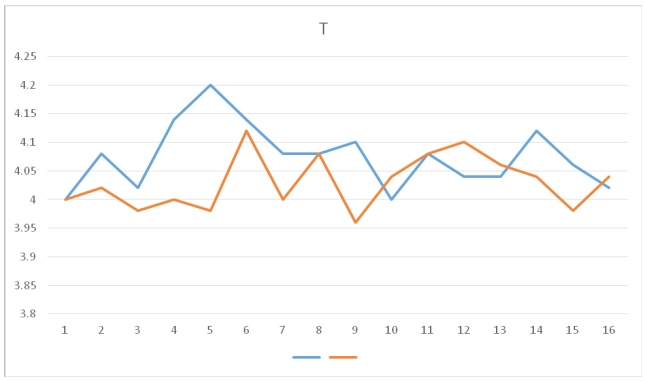

Figure 8. Thickness of SLA and SLS specimens.

Table 7. Standard deviation, dimensional change rate and dimensional accuracy of SLS

Tests	Std. Deviation (mm)	D. C. R. (%)	D. A. (%)
LO (Overall Length)	0.227968	0.0533	0.0533
WO (Overall Width)	0.078631	-0.232	0.0232
W (Width of Narrow Section	0.042404	-0.578	0.0578
T (Thickness)	0.048873	0.8	0.8

Figure 8 shows the variation of Thickness (T) measurements for the 15 samples of SLA and SLS each. There is considerable variation in the T measurements of both SLA and SLS specimens, SLA being lesser accurate than SLS in this case as well. The statistical and graphical data shows that the Dimensional Accuracy of SLS [**0.23**] is better than that of SLA [**0.94**]**.** It is also observed that both SLS and SLA specimens exhibit greater dimensional error in the smaller dimensions W (Width of the smaller section) and T (Thickness). This could be due to warping of the product due to the post- production curing process, or due to the machines inability to maintain its accuracy while printing smaller dimensions. However, even in these, the SLS specimens prove to be more accurate.

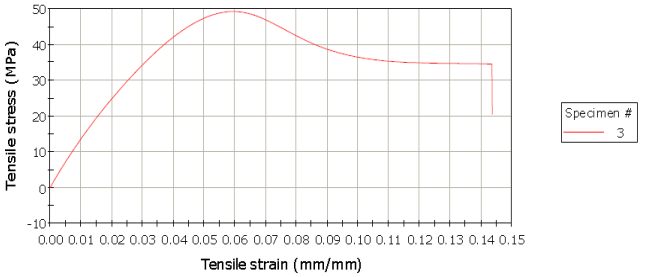

Figure 9. Stress-Strain Curve obtained by tensile testing of SLA specimen.

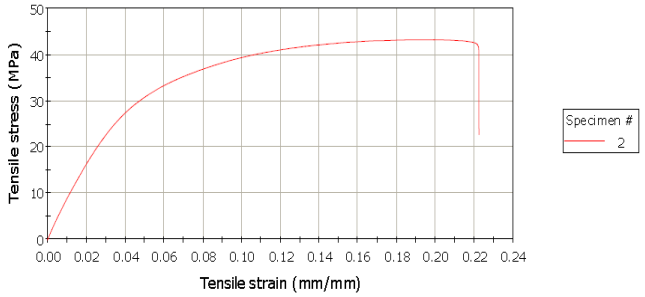

Figure 10. Stress-Strain Curve obtained by tensile testing of SLS specimen.

3.2 Tensile Strength Test

Five specimens each of SLA and SLS were tested on the INSTRON 3366 testing machine in this experiment. The values of elongation in mm, tensile stress and tensile strain were calculated with increasing values of longitudinal load. The values obtained were plotted to obtain a stress-strain curve and the modulus of elasticity was calculated (Figure 9 and 10). These details can be found in Table 8. Observation of the Stress-Strain trends show that the curve for the SLA specimens rises to a peak and then drops lower before reaching the break and failure point. However, the curve for the SLS specimen's rises almost linearly before reaching the break and failure point. This may imply that the SLS specimens are more rigid than the SLA specimens, which may be an undesirable property for a material used in rapid prototyping. It is observed that the average elongation of SLA specimens (3.123956 mm) is less than that of SLS specimens (6.09806 mm). The tensile stress of SLA specimens (48.423608 Mpa) is greater than that of SLS specimens (35.40161 Mpa). It can thus be concluded that SLA specimens outperform the SLS specimens in the Tensile Strength Test. It was also observed that the experimentally obtained values of Tensile Stress and Elongation conform to the expected values in both, the Accura-60 Plastic used for SLA and the DuraForm PA Plastic used for SLS. It must be noted that there was a larger elongation in the SLS specimens as compared to the SLA specimens, which is quite undesirable in terms of dimensional stability under loading.

Table 8. Average values of elongation, max. tensile stress, load at max. tensile stress, tensile extension and elasticity modulus for SLA and SLS specimens

Tests	SLA	SLS
Avg. elongation	3.123956 mm	6.09806 mm
Avg. max. tensile stress	48.4233608 MPa	35.40161 MPa
Avg. load at max. Tensile stress	1249.32912 N	1047.52167 N
Tensile extension	1.459416 mm	5.19673 mm
Avg. elasticity modulus	1322.20325 MPa	645.39296 MPa

3.3 Water Absorption Test

Five specimens of SLA and SLS each were placed in beakers filled with distilled water for a duration of 24 hours. The set up was maintained at a temperature of around 32 °C. After the desired time period, the specimens were gently cleaned and weighed on the Infra Digital IN 2011 weighing balance. The weights of the specimen before and after immersing in water are as shown in Table 9. Using this data, the percentage of water absorbed was calculated using the formula:

$$Percentage\ of\ water\ absorbed = \left\{\frac{Weight\ of\ specimen\ after\ test\ (g) - Initial\ weight(g)}{Initial\ weight(g)}\right\} \times 100 \quad \%$$

Table 9. Data collected for water absorption test of SLA and SLS specimens

Sr. No	Type	Weight After Test (g)	Initial Weight (g)	% Water Absorption
1	SLA	8.288	8.23	0.704738761
2	SLA	8.32	8.228	1.118133204
3	SLA	8.282	8.255	0.3270745
4	SLA	8.227	8.13	1.193111931
5	SLA	8.294	8.238	0.679776645
1	SLS	6.506	6.368	2.167085427
2	SLS	6.095	6.022	1.212221853
3	SLS	6.124	5.976	2.476572959
4	SLS	6.044	6.03	0.232172471
5	SLS	6.425	6.193	3.746165025

The average percentage of water absorbed by SLA specimens is 0.804567%. The average percentage of water absorbed by SLA specimens is 1.966844%. The SLA specimens were made from Accura–60 polymer which is a liquid photosensitive material, and the SLS specimens were made from Duraform PA powdered raw material. Since liquid homogenously occupies the entire space it is placed in, it is expected to have minimal void gaps in its structure[46]. This proved to be true in the case of the Rapid Prototyping specimens as well. The layers of sintered liquid polymers in the SLA specimens were more compact and thus allowed minimal water absorption. On the other hand, the SLS specimens allowed water to enter more freely into their granular structure, thus trapping a considerably larger amount of water in them. In case of the SLS specimens, the increase in weight of the specimens after immersing in water could be felt by human inspection. It was observed after the test that the SLA specimens absorbed 0.804567% by weight of water on an average, while the SLS specimens absorbed more than twice that amount i.e. 1.966844% by weight of water on an average.

3.4 Density Test

The density test was conducted according to the Archimedes Principle. Ten specimens each of SLA and SLS were immersed in water and the volume of water they displaced was calculated. The weight of the specimens was also calculated on the Infra Digital IN 2011 digital weighing scale. This was used to calculate the density of the specimens. The weights, volume of water displaced and density of the respective specimens are shown in Tables 10 and 11. The density of specimens was calculated using the following formula:

$$Density = \frac{Mass\ (kg)}{Volume\ (m^3)} \quad kg/m^3$$

Table 10. Data collected for density test of SLA specimens

Type	Sr. No.	Mass kg	Volume 10^{-6} m^3	Density kg/m^3
SLA	1	0.00823	6.736	1221.7933
SLA	2	0.00823	6.62	1242.9003
SLA	3	0.00826	6.843	1206.3422
SLA	4	0.00824	6.899	1194.0861
SLA	5	0.00813	6.831	1190.1625
SLA	6	0.00821	6.707	1223.6469
SLA	7	0.00817	6.724	1214.6044
SLA	8	0.00823	6.749	1219.2917
SLA	9	0.00819	6.609	1238.4627
SLA	10	0.00819	6.717	1219.4432

Table 11. Data collected for density test of SLS specimens

Type	Sr. No.	Mass kg	Volume 10^{-6} m^3	Density kg/m^3
SLS	1	0.00637	6.625	961.208
SLS	2	0.00602	6.51	925.038
SLS	3	0.00598	6.592	906.553
SLS	4	0.00619	6.558	944.343
SLS	5	0.00603	6.773	890.3
SLS	6	0.0061	6.592	925.061
SLS	7	0.00609	6.683	910.968
SLS	8	0.00604	6.543	923.735
SLS	9	0.00644	6.637	970.318
SLS	10	0.00597	6.718	888.806

The density test provides confirmation and reasoning to some of the other tests conducted such as dimensional accuracy test, tensile strength test, water absorption test and microscopy analysis. In the density test, it was

observed that the SLA specimens had an average density of 1217.0733 kg/m^3 while the average density of SLS specimens was 924.633 kg/m^3. The SLA specimens have a greater density than the SLS specimens. When objects of higher density undergo a phase change, they undergo a greater amount of volume change. This could explain the lower dimensional accuracy of SLA specimens as compared to SLS specimens. Also, denser objects exhibit better tensile strength, which is why SLA specimens proved to be stronger than the SLS specimens in the tensile strength test. Since the SLS specimens have a lower density, but approximately same space volume as the SLA specimens, this means that they have a greater amount of void spaces in their structure. Since the SLS specimens are made of granular composition, they absorbed a greater amount of water than the SLA specimens, which were more densely packed. Lastly, the microscopy analysis reveals the structure of the SLA and SLS specimens under a microscope, and thus confirms their difference in density.

3.5 Surface Roughness Test

The instrument used was the Mitutoyo SurfTest SJ-301 surface testing machine. The set up consisted of a diamond-tipped probe that was made to travel a sample length of 4 mm on the specimen's surface. The instrument calculated the arithmetic average value of Surface Roughness (R_a), Root Mean Square value of surface roughness (R_q) and the average distance between the highest peak and lowest valley in the sample length (R_z). For simplicity of purpose, only the R_a value of surface roughness has been considered in this project. Five samples of SLA and SLS each were tested for surface roughness and two readings were taken for each sample. The R_a values obtained are shown in Table 12.

Table 12. Data collected for surface roughness test of SLA and SLS specimens

Type	Sr. No.	R_a 1 µm	R_a 2 µm	Type	Sr. No.	R_a 1 µm	R_a 2 µm
SLA	1	3.23	2.22	SLS	1	11	5.59
SLA	2	0.37	0.69	SLS	2	15.58	15.91
SLA	3	0.63	1	SLS	3	16.87	16.09
SLA	4	0.85	0.67	SLS	4	10.21	12.72
SLA	5	1.54	1.17	SLS	5	19.24	10.27

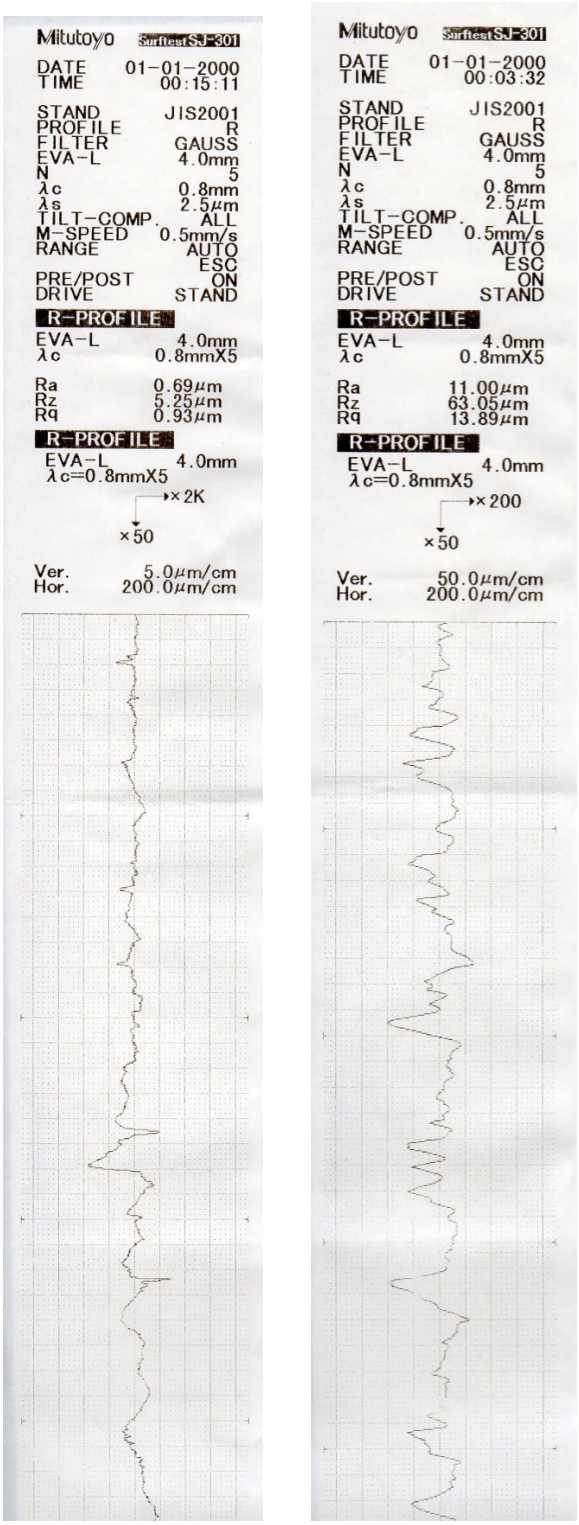

(a) (b)

Figure 11. Surface roughness parameters and roughness (R_a) plots for (a) SLA specimen and (b) SLS specimen.

The average surface roughness of SLA specimens was found to be 1.237 µm. The average surface roughness of SLS specimens was found to be 13.348 µm. As seen from Table 12 the SLA specimens have an average surface roughness of 1.237 µm as compared to that of the SLS specimens being almost 20 times that amount, i.e. 13.348 µm. Thus the surface of specimens manufactured by SLA is much better than those manufactured by SLS. This can be seen graphically in the plot of surface roughness printed by the SurfTest SJ-301 instrument, which is seen in Figure 11.

3.6 Vickers Hardness Test

The Vickers hardness test was conducted using 3 samples each of SLA and SLS. Three readings were conducted on each specimen, using the Matsuzawa MMT-X7A Vickers hardness testing machine. The readings obtained are shown in Table 13. It is observed that the average hardness number of the Stereolithography (SLA) specimens is 12.1333 and the average hardness number of the Selective Laser Sintering (SLS) specimens is 14.1889. The SLS specimens were thus proven to be harder than the SLA specimens by a small amount. The solid nature of raw material could be the reason behind the greater hardness of the SLS specimen.

Table 13. Vickers hardness number values of SLA and SLS specimens

Type	Sr. No.		Vickers hardness number		Avg. hardness number
		1	**2**	**3**	
SLA	1	13.1	13.1	13	
SLA	2	10.8	10.7	10.8	12.1333
SLA	3	12.6	12.6	12.5	
SLS	1	13.8	13.9	13.8	
SLS	2	14.5	14.6	14.5	14.1889
SLS	3	14.2	14.2	14.2	

3.7 Microscopy Analysis

Microscopy analysis was conducted to examine the structure and particular nature of the SLA and SLS specimens. The specimens were cleaned and placed on the objective slot of the METJI MSHOT M 1004 Trinocular Inverted Metallurgical Microscope, which was used to obtain images of the specimen's compositional attributes. The specimens used included fresh specimens and specimens that had undergone the tensile test and water absorption test. The test recorded images of the flat surface, failure region of tensile specimens as well as the flat surface of the water soaked specimens. Magnifications used were 50× for the flat surfaces of dry and wet specimens, and 200× to examine the failure region of the specimens subjected to tensile testing. The images obtained are shown in Figures 12 to 16.

Figure 12 shows the images of the SLA specimen's structure when observed on its flat surface. As known, the SLA process involves solidification of the liquid polymer by the action of a laser beam. Due to this process, the incremental layers of material deposited are observed to be linear and uniform. Figure 13 shows the images of the SLA tensile testing specimen's failure region. Since the specimens have been created from a liquid polymer, it exhibits typical brittle crystalline structure in the fail-

Table 14. Compilation of results of all tests conducted on the SLA and SLS specimens

RP system	Dimensional accuracy %	Tensile properties		
		Tensile stress	Tensile elongation	
		MPa	mm	
SLA	0.94	42.4233608	3.123956	
SLS	0.23	35.40161	6.09806	
RP system	**Water absorption %**	**Density kg/m³**	**Surface roughness µm**	**Vickers hardness number**
SLA	0.804567	1217.0733	1.237	12.1333
SLS	1.966844	924.633	13.348	14.1889

ure zone. The break is comparatively clean and smooth as compared to the failure region exhibited by the SLS specimens. Figure 14 shows the images of the SLS specimen's structure when observed on its flat surface. As known, the SLS process involves the sintering of powdered granular raw material by the action of a laser beam. Due to this process, the incremental layers of material are observed to be granular and rough. Figure 15 shows the images of the SLS tensile specimen's failure region. Since the specimens have been created from powder raw material, it exhibits characteristics similar to amorphous materials in the failure zone. The break is rough, and the granules cannot be identified individually, unlike the flat SLA specimen image in Figure 12. Figure 16 shows images of the SLA and SLS specimens that were subject to water absorption testing. Unlike Figure 12, the SLA specimen exhibits higher water retention and glossiness. The distance between the consecutive incremental layers seems greater. Also, the SLS specimen in Figure 16 shows considerably water retention and the granules seem bloated and surrounded by water.

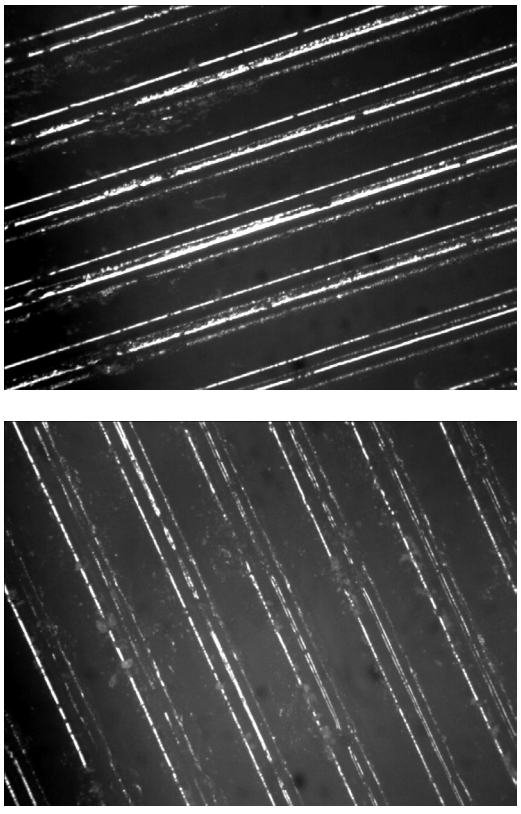

Figure 12. Microscopic images of flat surface of SLA specimens.

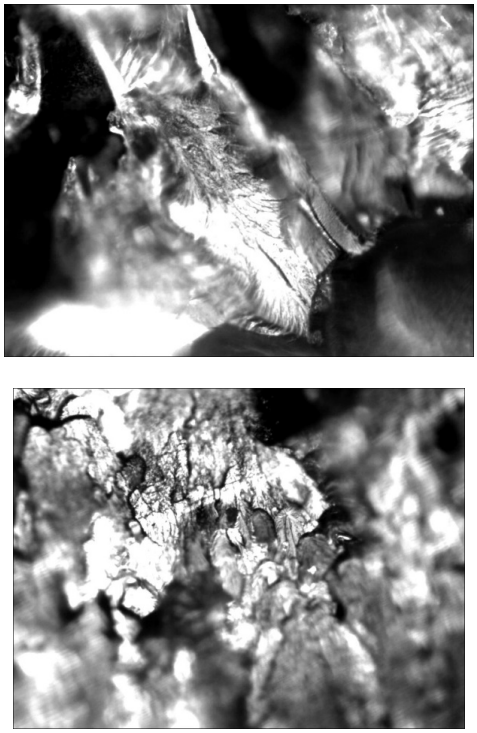

Figure 13. Microscopic images of failure region of SLA tensile testing specimens.

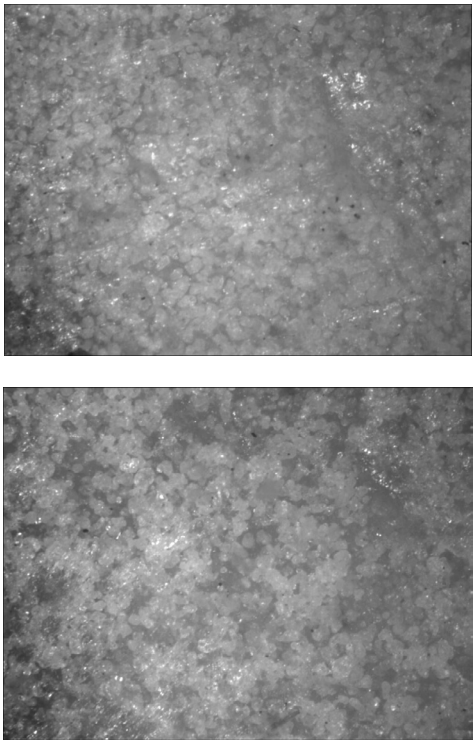

Figure 14. Microscopic images of flat surface of SLS specimens.

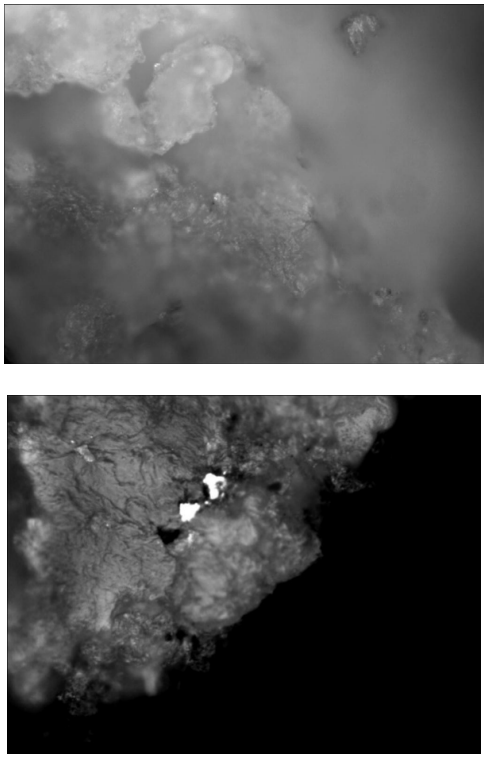

Figure 15. Microscopic images of failure region of SLS tensile testing specimens.

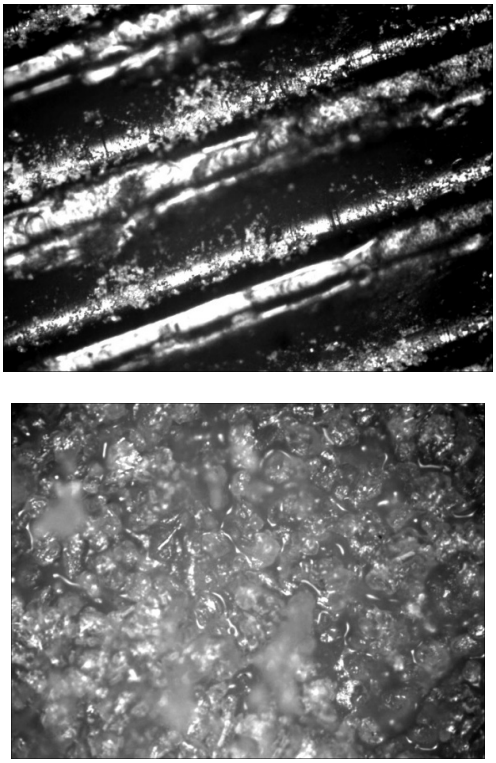

Figure 16. Microscopic images of water absorption test specimens of (a) SLA and (b) SLS.

4. Conclusions

This research compares the SLA and SLS specimens on the parameters of dimensional accuracy, tensile strength, water absorption, density, surface roughness and microscopic structure. As seen above, the SLS is better than SLA in dimensional accuracy. However, SLA is better than SLS in the parameters of tensile strength, water absorption, density and surface roughness. Thus it can be clearly inferred that the SLA specimens proved to be better than the SLS specimens in the scope of our research. The SLA specimens were manufactured from the liquid photopolymer Accura 60. Since the raw material was liquid, its molecular structure is more compact, which is why the SLA specimens performed better in the density, tensile strength, and water absorption tests. The SLS specimens were made using solid powdered raw material DuraForm PA. The nature of raw material enabled the SLS specimens to be geometrically more precise, thus performing better in the dimensional accuracy test. Also, the uniformity and smoothness of surface obtained from solidified liquid is much greater than that obtained by fusing individual powdered granules. Thus the surface roughness of the SLA specimens proved to be better than that of the SLS specimens.

This research in the field of rapid prototyping can be furthered by testing and experimenting with other parameters such as effect of heat of specimens[47], effect of variation of laser intensity and efficiency[48], variation of bed temperature, variation of fabrication parameters[49,50], multi-powder delivery[51], type of raw material and their combinations[52] etc. that can be conducted to make this research more comprehensive.

5. References

1. Yongnian Y, Shengjie L, Renji Z, Feng L, Rendong W, Zhuo LQX, Xiaohong W. Rapid prototyping and manufacturing technology: principle, representative technics, applications, and development trends. T singhua Science and Technology. 2009 Jun; 14(S1):1–12.
2. Upcraft S, Fletcher R. The rapid prototyping technologies. Assembly Automation. 1980; 23(4): 318–20.
3. Tiwari SK, Pande S, Agarwal S, Bobade SM. Selection of selective laser sintering materials for different applications. Rapid Prototyping Journal. 1995; 21(6):630–48.
4. Kochan A. Rapid developments in rapid prototyping. Assembly Automation. 1980; 15(4):18–19.

5. Chuk RN, Thomson VJ. A comparison of rapid prototyping techniques used for wind tunnel model fabrication. Rapid Prototyping Journal. 1995; 4(4):185–96.
6. Gunther D, Heymel B, Günther JF, Ederer I. Continuous 3D-printing for additive manufacturing. Rapid Prototyping Journal. 1995; 20(4):320–27.
7. Sambu S, Chen Y, Rosen DW. Geometric tailoring: A design for manufacturing method for rapid prototyping and rapid tooling. Journal of Mechanical Design, ASME. 2004 Jul; 126(4):1–571.
8. Patterson AM, Bibb R, Campbell RL, Bingham G. Comparing additive manufacturing technologies for customised wrist splints. Rapid Prototyping Journal. 1995; 21(3):230–43.
9. Raju BS, Sekhar UC, Drakshayani DN. Studies on application of rapid prototyping for the generation of photoelastic models and experimental analysis. IJAIEM. 2013 Feb; 2(2):1–7.
10. Gibson I, Kvan T, Ming LW. Rapid prototyping for architectural models. Rapid Prototyping Journal. 1995; 8(2):91–5.
11. Schiller GJ. Additive manufacturing for aerospace. IEEE Aerospace Conference; Big Sky, MT. 2015. 1–8.
12. Dawes WN. Rapid prototyping design optimization using flow sculpting. ASME Journal of Turbomachinery. 2008 Jul; 130(3):1–6.
13. Azari A, Nikzad S. The evolution of rapid prototyping in dentistry: A review. Rapid Prototyping Journal. 1995; 15(3):216–25.
14. Rahmati S, Dickens P. Stereolithography for injection mould tooling. Rapid Prototyping Journal. 1995; 3(2):740–7.
15. Lipson H, Moon FC, Hai J, Paventi C. 3D printing the history of mechanisms. ASME Journal of Mechanical Design. 2005 Sep; 127:1–22.
16. Cho U, Dutson AJ, Wood KL, Crawford RH. An advanced method to correlate scale models with distorted configurations. Journal of Mechanical Design, ASME. 2005 Jan; 127(1):78–85.
17. Lifton VA, Lifton G, Simon S. Options for additive rapid prototyping methods (3D printing) in MEMS technology. Rapid Prototyping Journal. 1995; 20(5):403–12.
18. Ivanova O, Williams C, Campbell T. Additive manufacturing and nanotechnology: Promises and challenges. Rapid Prototyping Journal. 1995; 19(5):353–64.
19. Deak SM. Safe work practices for rapid prototyping. Rapid Prototyping Journal. 1995; 5(4):161–3.
20. Conley JG, Marcus HL. Rapid prototyping and solid free-form fabrication. ASME Journal of Manufacturing Science and Engineering. 1997 Nov; 119:1–6.
21. Karalekas D, Rapti D. Investigation of the processing dependence of SL solidification residual stresses. Rapid Prototyping Journal. 1995; 8(4):243–7.
22. Phatak AM, Pande SS. Optimum part orientation in rapid prototyping using genetic algorithm. IEEE Journal of Manufacturing Systems. 2012; 31:395–402.
23. Peres F, Martin C. Design methods applied to the selection of a rapid prototyping resource. In: 7th IEEE International Conference on Emerging Technologies and Factory Automation; Barcelona; 1999. 1:417–22.
24. Borille A, Gomes J, Meyer R, Grote K. Applying decision methods to select rapid prototyping technologies. Rapid Prototyping Journal. 1995; 16(1):50–62.
25. Punyamurthy R, Sampathkumar D, Bennehalli B, Patel GR, Gouda R, Srinivasa VC. Pre-treatments on mechanical characterization of natural abaca epoxy composites. Indian Journal of Science and Technology. 2015 Jun; 8(11):1–11.
26. Monfared V, Hassan M, Danshmand S, Taheran F, Ghaffarivardavagh R. Effects of geometric factors and material properties on stress behavior in rotating disk. Indian Journal of Science and Technology. 2014 Jan; 7(1):1–6.
27. Jager PJD, Broek JJ, Vergeest JSM. A comparison between zero and first order approximation algorithms for layered manufacturing. Rapid Prototyping Journal. 1995; 3(4):144–9.
28. Wei W, Xiaofeng S. Functionally gradient material laser rapid prototyping technique. Tsinghua Science and Technology. 2009 Jun; 14(S1):192–9.
29. Bugeda G, Cervera M, Lombera G, Onate E. Numerical analysis of stereo lithography process using finite element method. Rapid Prototyping Journal. 1995; 1(2):13–23.
30. Boboulos M. CAD-CAM and rapid prototyping application evaluation. 1st ed, 2010.
31. Senthilkumaran K, Pande PM, Rao PVM. Statistical modeling and minimization of form error in SLS prototyping. Rapid Prototyping Journal. 1995; 18(1):38–48.
32. Mueller J, Shea K, Daraio C. Mechanical properties of parts fabricated with inkjet 3D printing through efficient experimental design. Materials and Design. 2015; 86:902–12.
33. Nancharaiah T, Nagabhushanam M, Nagendram BA. Process parameters optimization in SLS process using design of experiments. IJMET. 2013 Apr; 4(2):156–62.
34. Chockalingam K, Jawahar N, Chandrasekhar U. Influence of layer thickness on mechanical properties in stereolithography. Rapid Prototyping Journal. 1995; 12(2):106–13.
35. Guan G, Hirsch M, Lu ZH, Childs DTD, Matcher SJ, Goodridge R, Groom KM, Clare AT. Evaluation of selective laser sintering process by optical coherence tomography. Materials and Design. 2015; 88:837–46.
36. Luo Y. Environmental performance analysis of solid freeform fabrication processes. In: Electronics and the Environment; Danvers, MA., 1999. 1–6.
37. Faludi J, Bayley C, Bhogal S, Iribarne M. Comparing environmental impacts of additive manufacturing vs traditional

machining via life-cycle assessment. Rapid Prototyping Journal. 1995; 21(1):14–33.
38. Chua CK, Leong KF, Lim CS. Rapid prototyping: Principles and applications. 3rd ed. 2010. P. 540.
39. Rajesh R, Anand MD. Prediction of EDM process parameters for a composite material using RBFNN and ANN through RSM. Indian Journal of Science and Technology. 2016 Apr; 9(13):1–12.
40. Rajesh R, Anand MD. Development of hybrid modeling and prediction of SR in EDM of AISI1020 steel material using ANFIS. Indian Journal of Science and Technology. 2016 Apr; 9(13):1–11.
41. Kai CC. Three dimensional rapid prototyping technologies and key development areas. IEEE Computing and Control Engineering Journal. 1994 Aug; 5(4):200–6.
42. Durham M, Grimm T, Rollins J. SLS and SLA: Different technologies for different applications, promotional literature. Austin, TX: Accelerated Technologies Inc. 1996.
43. Antonio A. Assessment of surface quality on textured FDM prototypes. Rapid Prototyping Journal. 2006; 12(1):35–41.
44. Kochan D, Kai CC, Zhaohui D. Rapid prototyping issues in the 21st century. Computers in Industry. 1999; 39(1):3–10.
45. Imaginarium (India) Pvt. Ltd. [Internet]. [cited 15 Feb 2016]; Available from: http://imaginarium.co.in/index.php.
46. 3D Systems Accura-60 Plastic (Brochure) for SLA. 2002.
47. 3D Systems DuraForm PA Plastic (Brochure) SLS. 2002.
48. 3D Systems Viper Si2 SLA Brochure. 2002.
49. 3D Systems SinterStation HiQ + HQ SLS Brochure. 2002.
50. Monzon M, Hernandez PM, Benitez AN, Marrero MD, Fernandez A. Predictability of plastic parts behaviour made from rapid manufacturing. Tsinghua Science and Technology. 2009 Jun; 14(S1):1–9.
51. Vail NK, Balasubramaniyan B, Barlow JW, Marcus HL. A thermal model of polymer degradation during selective laser sintering of polymer coated ceramic powders. Rapid Prototyping Journal. 1995; 2(3):24–40.
52. Yang Y, Loh HT, Fuh JYH, Wang YG. Equidistant path generation for improving scanning efficiency in layered manufacturing. Rapid Prototyping Journal. 1995; 8(1):30–7.